

B. TECH. PROJECT REPORT
On
FABRICATION AND REDUCTION OF
THERMAL DEGRADATION IN
PEROVSKITE SOLAR CELL

BY
GARVIT SHARMA, YASH R. SHINDE



DISCIPLINE OF METALLURGY ENGINEERING AND
MATERIAL SCIENCE
INDIAN INSTITUTE OF TECHNOLOGY INDORE

DECEMBER, 2019

FABRICATION AND REDUCTION OF THERMAL DEGRADATION IN PEROVSKITE SOLAR CELL

A PROJECT REPORT

*Submitted in partial fulfillment of the
requirements for the award of the degrees*

of

BACHELOR OF TECHNOLOGY

in

METALURGY ENGINEERING AND MATERIAL SCIENCE

Submitted by:

GARVIT SHARMA, YASH R. SHINDE



INDIAN INSTITUTE OF TECHNOLOGY INDORE
DECEMBER, 2019

CANDIDATE'S DECLARATION

We hereby declare that the project entitled “**Fabrication and Reduction of Thermal Degradation in Perovskite Solar Cell** ” submitted in partial fulfillment for the award of the degree of Bachelor of Technology in ‘**Metallurgy Engineering and Material Science**’ completed under the supervision of **Dr. Parasharam M. Shirage**, Associate Professor, Head, Discipline of MEMS IIT Indore is an authentic work.

Further, we declare that we have not submitted this work for the award of any other degree elsewhere.

Garvit Sharma, Yash R. Shinde

CERTIFICATE by BTP Guide

It is certified that the above statement made by the students is correct to the best of my knowledge.

Dr. Parasharam M. Shirage

Preface

This report on “Fabrication and Reduction of Thermal Degradation in Perovskite Solar Cell” is prepared under the guidance of Dr. Parasharam M. Shirage.

In this work we have tried to mainly achieve two objectives. The first one is to fabricate Perovskite Solar Cell in ambient conditions while maximizing the efficiency of the same. We have tried incorporating some techniques which are required and relevant for this objective.

The second objective is to minimize the effects which causes the degradation of Solar Cell. In order to achieve this objective, special emphasis has been given to degradations caused due to thermal effects. We have incorporated some materials which reduces the thermal effects and helps us to maximize the efficiency.

We have tried to the best of our ability and knowledge to explain the content in a lucid manner. We have added various figures and graphs to make it more illustrative.

Garvit Sharma, Yash R. Shinde

B.Tech. IV Year

Discipline of Metallurgy Engineering and Material Science

IIT Indore

Acknowledgements

We would like to express our sincere gratitude to our project supervisor Dr. Parasharam M. Shirage for his constant support in our B Tech project and related research, for his constant encouragement, patience, motivation and immense knowledge

We would also like to express our deepest gratitude to our Director sir, Dr. Pradeep Mathur for providing all the facilities and giving us the opportunity to work in a nice and conducive environment.

We would also like to express our deepest gratitude to all the AFMRG lab members for constant motivation and support.

It is because of their help and support, due to which we were able to complete the design and technical report.

Without their support this report would not have been possible.

Garvit Sharma, Yash R. Shinde

B.Tech. IV Year

Discipline of Metallurgy Engineering and Material Science

IIT Indore

Abstract

Persistent R&D to get alternatives to the market-dominating expensive & heavy silicon solar cells has led to the development of thin film technologies, one of which is perovskite solar cells (PSC). After being introduced in 2009 they have shown an unprecedented increase in efficiency – from <10% in 2012 to over 23% in just seven years. These solar cells can be manufactured with less energy and toxic material than traditional silicon solar cells.

On the downside, PSCs have stability challenges with all major environmental stress factors namely oxygen, humidity, light and temperature. The purpose of this project is to produce high-performance perovskite solar cells and make them more robust to different environmental degradation factors, especially thermal degradation.

We started by formation of a uniform coating of TiO_2 on fluorine doped tin oxide glass, and then further coating it with a mesoporous layer of TiO_2 . On further extensive literature survey, we found out that mesoporous layer of TiO_2 was hindering the flow of electrons, and hence would've resulted in lesser efficiency. So we decided to replace the mesoporous layer of TiO_2 with nanorods of TiO_2 grown with the help of hydrothermal deposition technique on top of the compact layer which was deposited earlier. In the recipe used for growth of TiO_2 nanorods on top of the compact layer, to observe the changes in the length of the nanorods, we varied the composition of the precursor, as well as the time for the process. While varying the composition, we took acid + DI water as 10ml + 30ml, 20ml + 20ml and 30ml + 30ml. While varying the time for hydrothermal deposition, we kept it for 6 hours, 8 hours, 15 hours 17 hours and 20 hours.

Then we fabricated NiO nanoparticles as HTL layer with the help of two different recipes.

List of Tables

Table no.	Title no.	Page
4.1	Heating Time Duration at 150°C	44
4.2	Parameters of cells with and without PMMA	45
4.3	Parameters for cells with and without PMMA heated at 50°C for different Time durations	47
4.4	Parameters for cells with and without PMMA heated 100°C for different Time durations	49

Abbreviations

PV	Photovoltaic
PSC	Perovskite Solar Cell
ITO	Indium Doped Tin Oxide
FTO	Fluorine Doped Tin Oxide
ETL	Electron Transport Layer
ETM	Electron Transport Material
HTL	Hole Transporting Layer
DI Water	De – ionized Water
NiCl ₂	Nickel Chloride
Ni(NO ₃) ₂	Nickel Nitrate
MaPbI ₃	Methyl Ammonium Lead Iodide
PMMA	Poly(methyl methacrylate)
FF	Fill Factor
Ti(OBu) ₄	Titanium Butoxide
NaOH	Sodium Hydroxide
IPA	Iso – propyl Alcohol
DMF	Dimethyl Formamide
DMSO	Dimethyl Sulfoxide
GBL	Gammabutyrolactone
ACN	Acetonitrile
CB	Chlorobenzene

Table of Contents

Candidate's Declaration

Supervisor's Certificate

Preface

Acknowledgements

Abstract

Abbreviations

1. INTRODUCTION

1.1 Solar Energy

1.1.1 Photovoltaic Effect

1.2 Perovskite

1.3 Hybrid Inorganic-Organic Perovskite

1.4 Degradation in Perovskites

1.5 Perovskites and Photovoltaics

1.6 Interface Engineering in PSCs using Polymer

1.7 Motivation

2. THEORY

2.1 Solar Cell Characteristics

2.2 Choosing the right layers for PSCs

2.3 Hysteresis in PSCs

3. EXPERIMENTAL TECHNIQUES

3.1 Cutting of FTO glass

3.2 Fabrication of Electron Transport Layer (ETL)

3.2.1 Preparation of TiO₂ solution

3.2.2 Preparation of TiO₂ nanorods

3.3 Fabrication of Hole Transporting Layer (HTL)

3.3.1 Preparation of NiO_x with NiCl₂ as precursor

3.3.2 Preparation of NiO_x with Ni(NO₃)₂ as precursor

3.4 Cell Fabrication for Degradation Controlled Properties

3.4.1 Materials Used

3.4.2 Solution Preparation

3.4.3 Deposition of the layers

4. RESULTS AND DISCUSSIONS

4.1 For Electron Transport Layer (ETL)

4.1.1 Fabrication of compact layer on FTO substrate

4.1.2 Fabrication of TiO₂ nanorods on top of the compact layer

4.2 For Hole Transport Layer (HTL)

4.2.1 By using Nickel Chloride (NiCl_2)

4.2.2 By using Nickel Nitrate $\text{Ni}(\text{NO}_3)_2$

4.3 Cell Fabrication for Degradation Controlled Properties Results

4.3.1 Adding a Layer of PMMA between Perovskite and NiO_x

4.3.2 Heating the substrate with and without PMMA for various Time

Durations at 50°C

4.3.3 Heating the substrate with and without PMMA for various time

Durations at 100°C

5. CONCLUSIONS AND FUTURE SCOPE

6. REFERENCES

CHAPTER 1

Introduction

1.1 Solar Energy

The electromagnetic radiations coming from the sun possess energy in the form of light and heat. This energy can be used directly or converted to other forms for utilization. The solar energy received on earth every day is 200,000 times more than the world's daily electricity generating capacity. Although the energy received is totally free but high costs of collection and storage prevent it from complete exploitation. Thermal and electrical energy are the two main forms of energy it can be converted to. Flat plate collectors are generally used to capture thermal energy which is then used for heating applications like water heaters and house heating. Solar energy is directly converted to electricity using photovoltaic cells and the phenomenon is known as the photovoltaic effect. The most common type of the material commercially used for PVs is silicon, cells produced from which are expensive and heavy. Persistent R&D to get alternatives to the market-dominating expensive & heavy silicon solar cells has led to the development of thin film technologies, one of which is perovskite solar cells which have shown remarkable growth in their efficiencies.

1.1.1 Photovoltaic Effect

When electromagnetic radiation is incident on a photovoltaic cell with photons of energy equal or greater than the energy bandgap, a voltage or electric current is generated in the cell and this is called photovoltaic Effect. The difference of energy between the valence band and conduction band in a material is called bandgap. The energy levels of electrons in the outermost orbitals form the valence band and conduction band is the energy level to which electrons excite for making the material

conductive. It is not occupied by any electron in the ground state. For organic semiconductors, this energy gap is described as the energy difference between the highest occupied molecular orbital (HOMO) and lowest unoccupied molecular orbital (LUMO). The energy required to excite an electron from HOMO to LUMO is specific to the material. The energy of electromagnetic radiation (E) is related to its wavelength (λ) by the following relation:

$$E = \frac{hc}{\lambda}$$

Where h is the Planck's constant and c is the speed of light. When the electrons absorb photons with energy greater than the material's energy gap, they are excited to LUMO from HOMO leaving holes behind. The internal electric field prevents the excited electron from recombining with the holes. This movement of electrons and holes generates the current and the energy band gap of the material produces the voltage.

1.2 Perovskite

In 1839 the crystal structure of Calcium Titanate was discovered by German mineralogist Gustav Rose and was named after Russian mineralogist Lev Perovski as "Perovskite". Since then all compounds with the same crystal structure are referred to as perovskites. The general chemical formula of perovskite is ABX_3 , where A and B are cations of different sizes and X is an anion. ABX_3 structure consists of corner-sharing $[BX_6]$ octahedra as shown in the fig. 1.1. The eight octahedra form a site in

the middle of the cube which is occupied by a cation with 12-fold coordination.

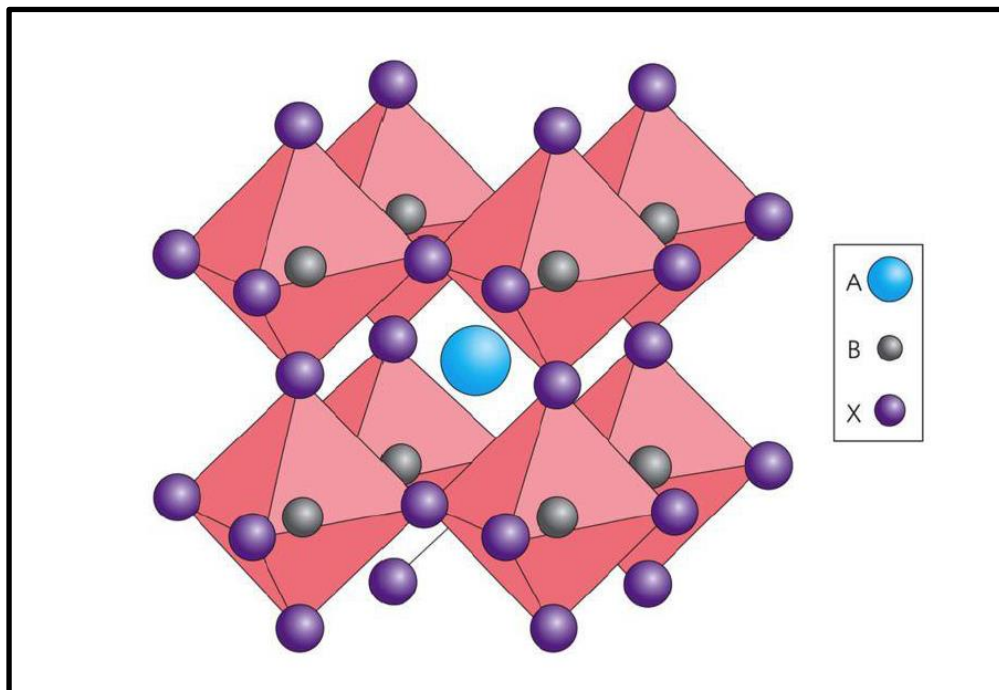


Figure 1.1 Structure of Perovskite ABX₃

The ideal structure of Perovskite illustrated in Fig. 1.1 has a cubic lattice although the unit cell of most perovskites is slightly distorted caused by different combinations of ion radii and steric constraints. Only SrTiO₃ possesses a perfect cubic unit cell.

In Perovskite structure, A or B lattice positions can be occupied by all the elements except noble gases. The ratio of ionic radii of A and B cations determines the stability of the structure. Not only size but the nature of A and B atoms determine the structure. If the “A” cation is monovalent, then the “B” cation must be divalent if “X” is a halogen and all sites are fully occupied.

In the generalized Perovskite structure ABX₃, on the basis of selected A, B & X keeping in mind the stable stoichiometry we can categorize perovskites as follows -

According to the representation of X

1. Oxide-based Perovskites: In these, X is represented by element Oxygen and A & B can be either inorganic or organic-inorganic compounds.
2. Halide-based Perovskites: Here X is represented by Halide ions (Cl^- , Br^- and I^-) and A & B are the same as Oxide-based. These are the most promising materials for PSCs.

According to the representation of A & B

1. Inorganic Perovskites: In these, both A & B are inorganic compounds e.g. CsSrI_3 .
2. Organic-inorganic (Hybrid) Perovskites: The most studied PSCs are organic-inorganic halide perovskites based in which A is a monovalent organic cation ($\text{CH}_3\text{NH}_3^+ = \text{MA}^+$, $\text{CH}(\text{NH}_2)_2^+ = \text{FA}^+$) but may also have some sites occupied by inorganic metal cation (Cs^+ and Rb^+), B is a divalent metal cation (Pb^{2+} , Sn^{2+} , Ge^{2+} , Mg^{2+} , and Ca^{2+}) and X is a halide ion, e.g. MAPbI_3 , FAPbI_3 .

1.3 Hybrid Organic - Inorganic Perovskite

It all started when in 2012; M. Grätzel and N. G. Park *et al.* made PSCs device using methylammonium lead iodide (MAPbI_3) perovskite films as the photoactive absorber layer and achieved an efficiency of 9.7% [9]. Although MAPbI_3 is considered as a great light harvester, it suffers from a harmful tetragonal–cubic phase transition at approximately 56 °C while the operational temperature of solar cells is considered up to 85 °C. Due to this phase transition, the band structure is affected and the band gap of MAPbI_3 due to Shockley-Queisser theory causes negative impacts on photovoltaic behavior. Due to all these issues, the attention is diverted to formamidinium lead iodide (FAPbI_3) [10, 11]. MAPbI_3 and FAPbI_3 have been extensively studied both theoretically and experimentally in recent years [12, 13]. The perovskites have become promising material for PSCs due to following advantages:

a) *Tunable Band Gap*: Shockley-Queisser (SQ) limit is the maximum theoretical value for efficiency of a solar cell using a single p-n junction. Rühle *et al.* [14] calculated it to be 33.7% at 1.34 eV. A study [15] has shown that varying the halide composition between iodide and bromide in the methylammonium trihalide system the bandgap can be tuned between 1.55 and 2.3 eV, which can be used for variation in color and for incorporating in multi-junction solar cells but for a single junction solar cell the optimal bandgap is between 1.1 and 1.4eV. Although by changing the size of A cation by using formamidinium narrows the bandgap to 1.48eV [16] bringing it closer to the ideal bandgap.

- a) Diffusion lengths exceed 1 μm for electrons and holes [17].
- b) Low- cost, easy and scalable manufacturing process.

1.4 Degradation in Perovskite

a) *Degradation due to moisture*: When exposed to humidity methylammonium based perovskites degrades which was recognized as the main extrinsic factor for degradation of PSCs. It exhibits intrinsic thermal instability due to its low formation energy and volatility of the organic cations [18, 19]. The formamidinium (FA)-based FAPbI₃ perovskite, although more thermally-stable than MAPbI₃, has both a photoactive trigonal α -phase and an undesired hexagonal δ -phase. The photoactive trigonal α -phase tends to convert to the δ -phase at room temperature, and this conversion is accelerated in the presence of moisture [20]. Although with a molecule passivated 3D/ Ruddlesden–Popper (R P) heterostructure Niu *et al* [21] achieved a PCE as high as 20.62% and remarkable long-term ambient stability with a t_{80} lifetime more than 2880 hours without encapsulation which is exceptional for PSCs but quite low when compared to 20000 hours lifetime of Silicon solar cells.

b) *Thermal degradation*: Typically, device temperatures can reach over 45°C higher than ambient temperatures when solar cells operate under direct sunlight. According to International Standard long-term stability at 85°C is required to compete with other solar cell technologies. Therefore, the study of the thermal stability of PSCs is utterly important for their commercialization. The surface of MAPbI₃ is degraded at a temperature as low as 85°C and the exact mechanism for degradation is still debated upon but the remarkable light harvesting properties of the material is lost over time because it degrades into PbI₂ after a little loss of MAI (CH₃NH₃I). This degradation from MAPbI₃ to PbI₂ is believed to occur by a release of gases i.e. ammonia & methyl iodide via simple sublimation. The first step during the thermal degradation of MAPbI₃ is shown in reaction 1 and the second reaction shows the further decomposition of MAI under an inert atmosphere which proceeds as:



After this NH₃ and CH₃ gases evaporate from the structure leaving only PbI₂ as residue. But Cs⁺ & formamidinium cations are the possible replacement for the methylammonium cation. Cesium lead halides & FA lead halides are stable up to temperatures of 300°C & 200°C [23, 24]. However, as mentioned above pure FAPbI₃ undergoes a phase transition to a hexagonal structure when cooled to room temperature called as δ -phase which is yellow & not photoactive. But by blending formamidinium with methylammonium this transition can be reduced to a great extent [25, 26].

1.5 Perovskite in Photovoltaics

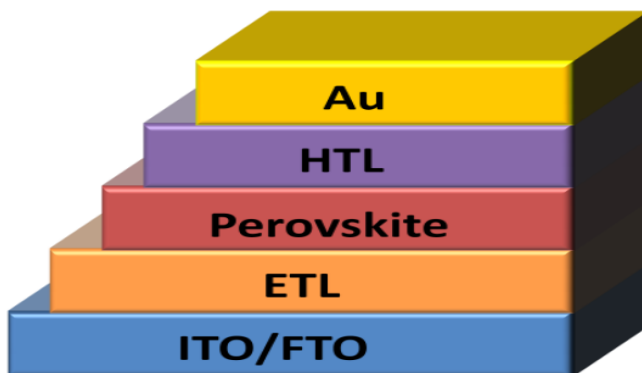


Fig 1.2 Basic layered structure of a PSC

The basic structure of a Perovskite solar cell is shown in Fig 1.2. The lowest layer is a transparent electrode which has ITO or FTO on a glass. The radiation first goes through this layer. Over it is the ETL, sometimes also called as electron collection layer where electrons enter from the absorber layer, transported through it and collected by the ITO/FTO. They are usually transition metal oxides (TiO₂, SnO₂, etc.) and metal oxide nanoparticles. On top of the

ETL is Perovskite which is the active layer where the incident photons are absorbed and an electron-hole pair is generated. On top of it is the HTL which extracts holes from the perovskite and lastly, there is a metal electrode usually made of gold on the very top. To create a closed circuit for operating the solar cell, the transparent and gold electrodes are connected with a load in between. When the radiation is incident upon the junction, the generated charge carriers flow through the circuit generating a photocurrent in the circuit and a voltage across the load.

1.6 Interface Engineering in PSCs using polymer

Formation of large pinholes has been observed in the perovskite layers [27] which can produce shunt-leakage thus reducing the photovoltaic performance. Because of these the HTL and ETL might come in direct contact and act as a parallel diode thus decreasing the open-circuit voltage and fill factor of the cells because of the increased recombinations. Also, degradation in the performance of the solar cells occurs due to non-radiative recombination losses caused by surface traps [28]. A compact layer of polymer like PMMA has been widely used to protect devices from oxygen and moisture [29]. Wang et al. reported an improvement in the photovoltaic performance and stability of MAPbI based PSCs with the use of a PMMA layer between the perovskite and the HTL layer [30].

1.7 Motivation

PSCs have stability challenges with all major environmental stress factors namely oxygen, humidity, light and temperature. Under operation, a solar cell is exposed to cyclic temperature variations during day and night which affect its performance. Studies have shown a temperature variation induced performance decline which is unique to PSCs. This is a major hindrance in their commercialization so to tackle this issue we plan to fabricate PSCs which are more stable when exposed to temperature variations. We plan to do this by using a standard PSC architecture ITO/ TiO₂/ Perovskite/NiOx/Au and add another layer of PMMA polymer which has already shown stability against moisture. This layer will be optimized to obtain a more temperature stable PSC.

CHAPTER 2

Theory

2.1 Solar Cell Characteristics

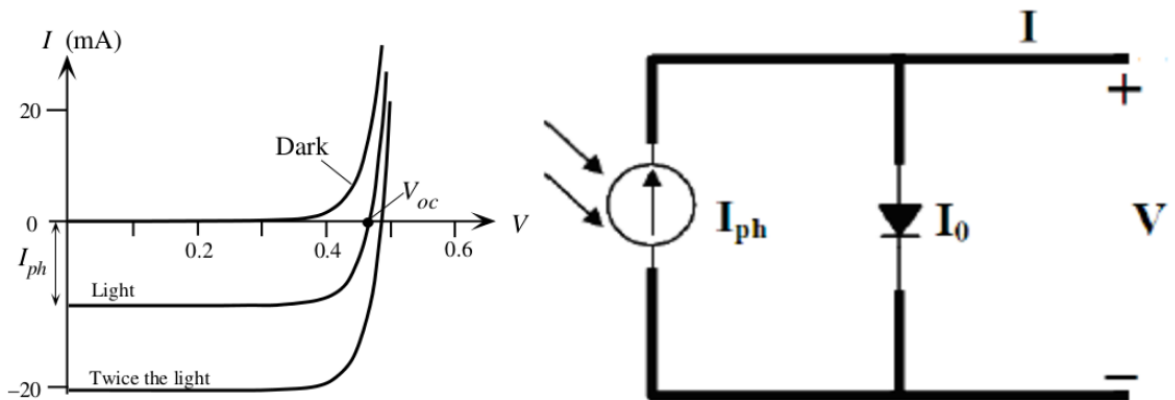


Fig 2.1 : (a) Equivalent circuit of a solar cell (b) I – V plot of a diode and a solar cell

Fig. 2.1(a) shows the equivalent circuit of a solar cell [31] and using Kirchoff's current law we can write:

$$I = I_0 - I_{ph}$$

Where I_0 is the diode current and I_{ph} is the photocurrent generated in the cell. So net current I is diode current decreased by an amount of photocurrent. We can see from the fig. 2.1(b) [31] that due to this decrease in this current the I-V curve is shifted to the fourth quadrant and now has a finite area under the curve. Since the area under the I-V curve gives power it tells us that now the power is generated from the solar cell. The photocurrent is directly proportional to the intensity of the incident light.

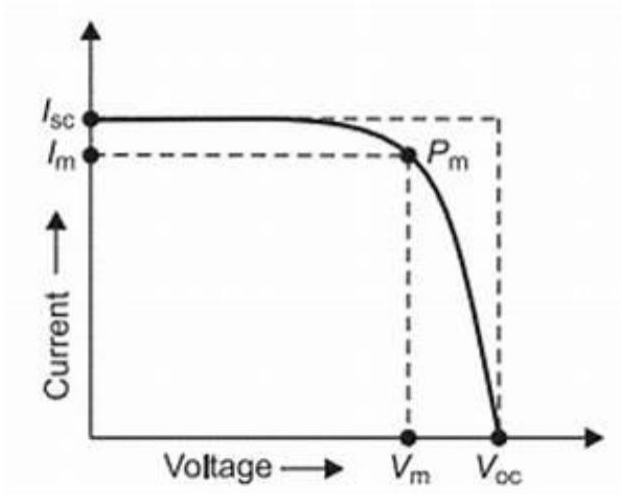


Fig 2.2 I – V plot of a solar cell indicating MPPs

From the fig. 2.2, Short circuit current (I_{sc}) is the current which flows through the circuit when the two electrodes of the cell are shorted making the voltage zero and open circuit voltage (V_{oc}) is the voltage across the cell when the circuit is open. The current and voltage value on the curve at which maximum power is generated from the solar cell is I_m & V_m and that point on the curve is called as a maximum power point (P_m). A solar cell is characterized by four parameters, two of them are I_{sc} & V_{oc} another two are fill factor & efficiency. Fill factor is given by

$$F.F = \frac{I_m V_m}{I_{sc} V_{oc}}$$

And efficiency is given by :

$$\eta = \frac{I_{sc} * V_{oc} * F.F}{E * A_c}$$

Where E is the incident flux and A_c is the active area of the cell.

2.2 Choosing the right layers for PSCs

The layers in perovskite solar cells are carefully chosen according to their band energy compared to the adjacent layers because when electrons are excited they will always try to minimize the energy by recombining with holes. But another property of the charge carriers is that they will always prefer the path of minimum resistance. So if the right layer structure is

chosen, recombination can be decreased if charge carriers are made to take a different route. This is done by selecting an ETL which is having its LUMO lower than the LUMO of perovskite thus making a more attractive way for an electron to go. The same idea applies for the selection of HTL in which its HOMO should be higher than the HOMO of perovskites creating a more attractive way for holes to go. The same concept should be applied to all the layers of the PSC for the chain transportation of the charge carriers to occur as shown in fig. 2.3.

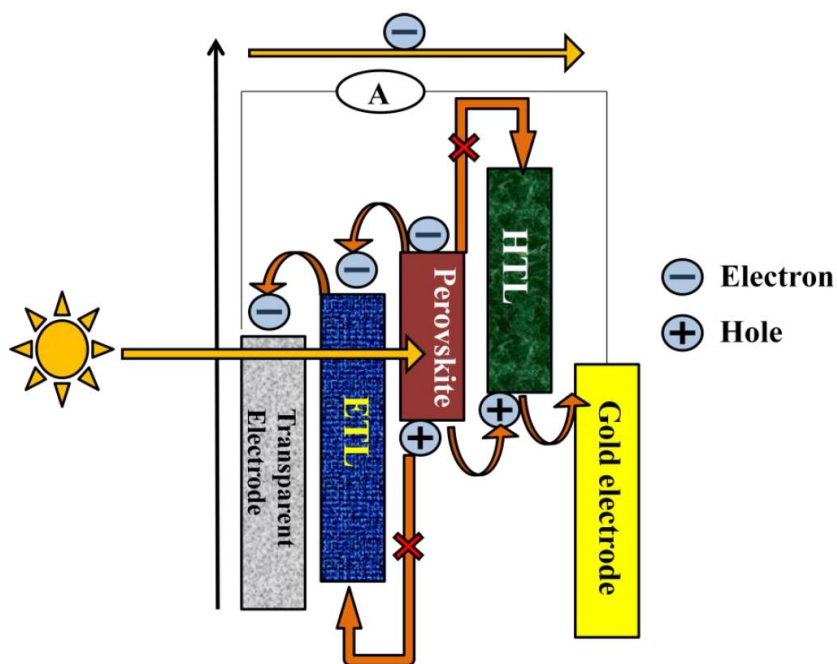


Fig 2.3 - Energy band diagram of PSC layers

2.3 Hysteresis in PSCs

For the JV characteristics measurement is done in two directions, starting from the maximum preset value voltage towards the minimum preset value called as backward direction or vice-versa which is the forward direction. In PSCs, these two curves do not overlap as shown in fig. 2.4.1 which in turn gives two different values for each cell parameter. This is called hysteresis in PSCs. One of the most accepted reasons for it to happen is the ion migration. Weber et al. proposed the following mechanism for explaining the hysteresis [32].

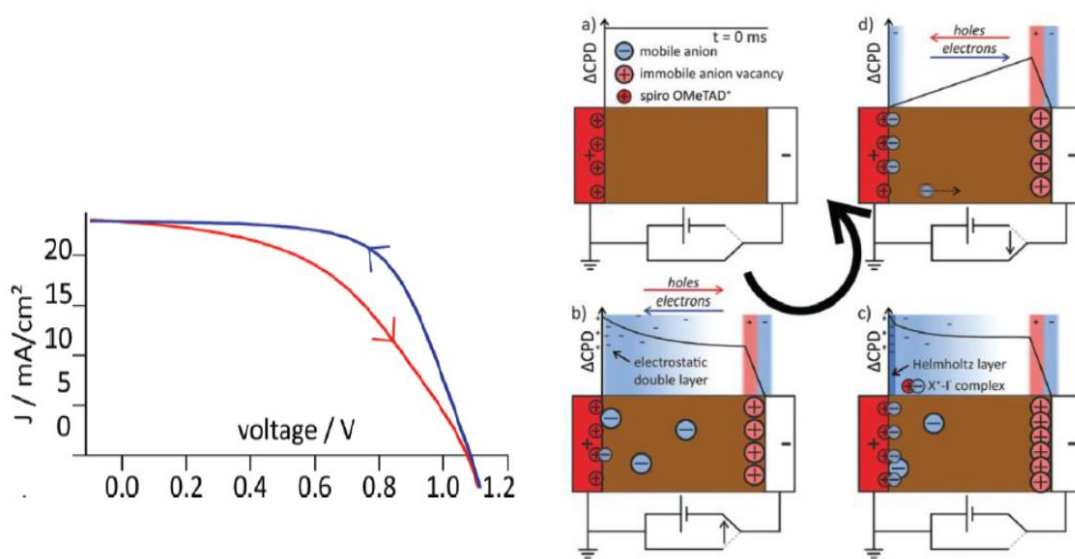


Fig 2.4 - (I) JV characteristics of a PSC showing hysteresis **(2)** Proposed mechanism of hysteresis: (a) The perovskite layer has no internal field in equilibrium (b) When an electric field is applied, it is screened by the mobile Iodide ions released from the perovskite at the anode interface and positive ions are adsorbed at the cathode interface. (c) The entire electric field is screened by these charges and the net potential across the perovskite layer becomes flat. (d)When the external field is switched off, this reverse internal electric field helps in driving electrons and holes towards the anode and cathode [32].

CHAPTER 3

Experimental Techniques

3.1 Cutting and cleaning of the FTO substrates

FTO coated glass come in 64mm x 64mm sheets which we cut into sixteen 16mm x 16mm substrates. Cleaning was performed in the following steps:

- 1.) Substrates were washed in DI water to remove any small glass pieces stuck to them.
- 2.) After that, they were ultrasonicated in acetone for 7 minutes and then dried with a nitrogen gun.
- 3.) In this step, they were again ultrasonicated with Ethanol for 7 minutes and dried with a nitrogen gun.
- 4.) In this final step, substrates were treated with oxygen plasma for 3 minutes.

3.2 Fabrication of Electron Transport Layer (ETL)

Materials: Cleaned glass with FTO coated on it, 0.15 M and 0.30 M TiO_2 , 37% HCL, Titanium Butoxide, DI Water, Acetone, Ethanol, titanium diisopropoxide bis(acetylacetonate).

3.2.1 Preparation of TiO_2 solution

TiO_2 solutions with molarity 0.15 M and 0.30 M were prepared by mixing 10ml of Ethanol with requisite amount of titanium diisopropoxide bis(acetylacetonate).

Spin Coating Technique

It is the most common technique used for depositing thin films on the substrates. The apparatus used for it is called a spin coater. It has the ability to produce thin uniform films easily with varying thickness from nanometer to micrometers in range. It is widely used in semiconductor industries and other technological areas.

Working Principle:

This technique uses centrifugal force to spread uniform films on flat substrates. A solution of materials is dispensed onto the center of the substrate, which is then rotated at high speed. Rotation is continued until the excess solution flung off the substrate and a film of desired thickness is achieved. Spin speed, acceleration, time of deposition and viscosity of the solution defines the film thickness. Evaporation rate of the solvent and wettability also affect the film quality. Although some part of the solvent evaporates while spinning but usually substrates are annealed to evaporate the residual solvent. There are two common methods of dispensing, static and dynamic. In static, the puddle of fluid is first dropped and then the substrate is spun but in dynamic the fluid is dispensed on a spinning substrate which is helpful when the fluid or substrate has poor wetting abilities.

Deposition of TiO₂ Compact Layer

The FTO glass was coated by 0.15 M TiO₂ once and by 0.30 M TiO₂ twice on top of the 0.15 M coating by spin coating at 4000 RPM for 30s (for both 0.15 M and 0.30 M). The substrates were then heated at 120°C for 30 minutes in ambient air conditions.

3.2.2 Preparation of TiO₂ Nanorods

Materials: Cleaned glass with FTO coated on it, 37% HCL, DI Water, Titanium Butoxide, teflon coated container, autoclave, Muffle Furnace.

Preparation of Precursor Solution.

A solution was prepared by mixing 30ml HCL and 30ml DI Water which was then stirred for 10 minutes. For preparing the precursor solution, 0.75ml of Titanium Butoxide (Ti(OBu)₄) was added to the acid solution, which was then stirred for around 10 minutes.

Hydrothermal Deposition

Hydrothermal synthesis can be defined as a method of synthesis of single crystals that depends on the solubility of minerals in hot water under high pressure. The crystal growth is performed in an apparatus consisting of a steel pressure vessel called an autoclave, in which a nutrient is supplied along with water. After keeping the substrate

in this solution for a specific time and at specific temperature, growth of nanorods of the nutrient supplied takes place. The growth depends on the composition of the solution, the temperature at which it is kept and the time for which it is kept.

Growth of TiO₂ nanorods

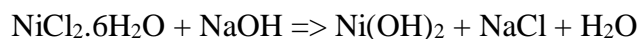
A solution was prepared by mixing 30ml of 37% HCL and 30 ml of DI Water which was then stirred for about 15 minutes. 0.75 ml of Titanium Butoxide (Ti(OBu)₄) was then added to the above mixture and rigorously stirred for 15 minutes. FTO glass coated with a compact thin film of TiO₂ was used as a substrate. This substrate was kept into the teflon coated container, the precursor solution prepared earlier was then poured into the container. This container was then tightly packed in a steel autoclave which was then kept in the furnace at 150°C for varying time intervals viz. 6, 8, 15, 17 hours.. The substrates were then removed from the autoclave and annealed at 500°C for 30 minutes.

3.3 Fabrication of Hole Transporting Layer (HTL)

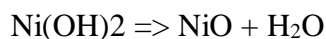
Materials: Nickel Chloride (NiCl₂), Nickel Nitrate (Ni(NO₃)₂), Sodium Hydroxide (NaOH), Ethanol, DI water, Butter paper, Analytical Weighing Balance, centrifuge machine.

3.3.1 Preparation of NiO_x with NiCl₂ precursor

1.5 gm NiCl₂ was dissolved in 70ml Ethanol and stirred rigorously for 10 minutes. 0.55 gm of NaOH was dissolved in 100ml Ethanol in another beaker and stirred for 5 minutes. The NaOH solution was added into the Nickel Chloride solution dropwise, while stirring the Nickel Chloride solution until the pH value reached 10. The reactions that occur in this process are as follows -



The solution thus formed was centrifuged in order to wash the solution and obtain Ni(OH)₂ gel. This was done for 15 minutes twice at 7000 RPM. The gel thus formed was subsequently heated at 750°C for 4 hours. The reaction that takes place in the furnace is as follows –



3.3.2 Preparation of NiO_x with Ni(NO₃)₂ precursor

0.5 mol $\text{Ni}(\text{NO}_3)_2$ was dispersed in 100ml of DI water to get a dark green solution. pH of this solution was then adjusted to be 10 by adding 10M NaOH solution dropwise. This solution was stirred for 5 minutes, and was then centrifuged in order to wash it with DI Water and Ethanol. The gel thus obtained was then dried by heating it at 80°C for 6 hours. The obtained green powder was then calcined at 270°C for 2 hours to obtain a dark black powder.

3.4 Cell Fabrication for Degradation Controlled Properties

3.4.1 Materials Used

120 nm thick ITO layer coated on glass ($15\Omega\text{m}^{-2}$ sheet resistance, Luminescence Technology, CAS: 50926-11-9), aqueous colloidal dispersion of SnO_2 nanoparticles 15 wt% (Alfa Aesar), 0.4mmol lead Iodide (TCI), Formamidinium Iodide (GreatCell Solar), Methylammonium bromide(GreatCell Solar), Methylammonium chloride((GreatCell Solar), Butylammonium bromide(GreatCell Solar), Butylammonium iodide(GreatCell Solar), all the following solvents are from Sigma Aldrich: acetone, IPA DMF, DMSO, ACN, GBL, CB were used without any purification, DI water, PMMA spiro-OMeTAD (Luminescence Technology), Lithium bis(trifluoromethanesulfonyl) imide, 4-tert-butylpyridine, gold nuggets.

3.4.2 Solution Preparation

- a) **SnO_2 :** Precursor solution with concentration of 2.04 wt% was prepared: by diluting colloidal dispersion of SnO_2 in DI water.
- b) **PbI_2 :** We prepared a 1.2M solution in a solvent mixture of DMF: DMSO 19:1(v/v). It was shaken and heated at 70°C until completely mixed and then left overnight for the particles to settle down. The solution was filtered just before use.
- c) **Standard cation solution:** 60mg Formamidinium Iodide, 6mg Methylammonium bromide, and 6mg Methylammonium chloride were mixed in 1ml IPA.
- d) **PMMA solution:** Two solutions with PMMA were prepared with concentrations 0.1mg/ml and 0.21mg/ml with CB as the solvent.
- e) **Spiro-OMeTAD solution:** 17.5 μL lithium bis(trifluoromethanesulfonyl) imide (520 mg mL^{-1} in acetonitrile) and 4-tert-butylpyridine (28.5 μL) were added with 80mg spiro-OMeTAD and dissolved in 1 mL chlorobenzene.

3.4.3 Deposition of the layers

- a) **SnO_2 :** This ETL was deposited on the substrate by spin coating at 4000RPM for 30s followed by annealing at 250°C for 30 minutes in ambient air condition (30-40% humidity). and oxygen plasma treatment for 1 minute.

b) **PbI₂**: We use a two-step process for spin coating perovskite. In this first step, PbI₂ was spin coated at 1500RPM for 30s and afterward annealed at 70°C for 1 minute in an inert atmosphere.

c) **Cation mixture**: This is the second step in which the cation solution was spin coated at 1300RPM for 30s in inert atmosphere followed by annealing at 150°C for 15 minutes in ambient air condition (30-40% humidity).

d) **PMMA**: We deposited it by dynamic dispensing for spin coating at 4000RPM for 30s followed by annealing at 80°C for 6 minutes in an inert atmosphere. Although its annealing was not performed in some experiments and directly Spiro-OMeTAD was coated over the perovskite.

e) **Spiro-OMeTAD**: This was spin coated at 4000RPM for 30s and left for oxidation in dry air for 12-14 hours.

f) **Contact swiping**: Edges of the substrate were swiped with GBL to remove the spin-coated layers and form contacts.

g) **Gold (Au) evaporation**: Au electrode with a thickness of 60nm was deposited by thermal evaporation through shadow masks to define the active area to 10.5 mm

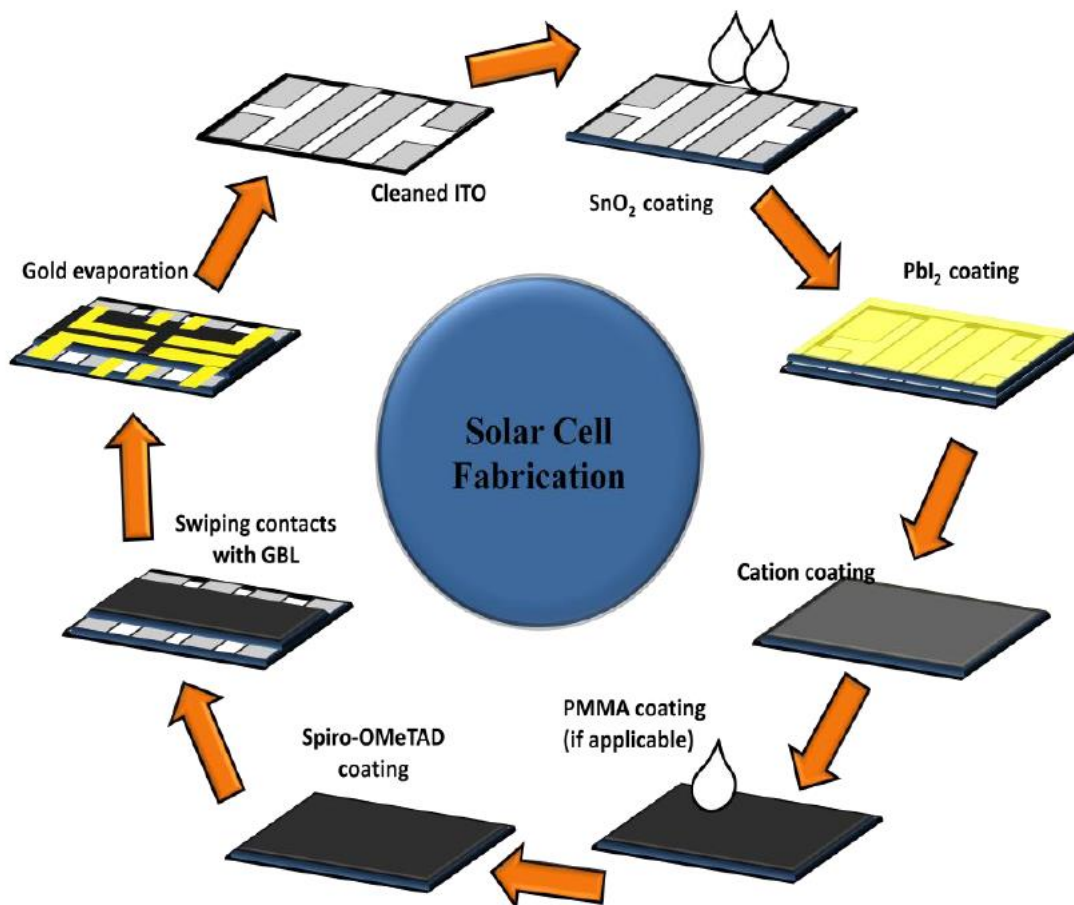


Fig 3.1 Fabrication of Solar Cell

CHAPTER 4

Results and Discussions

4.1 For Electron Transport Layer (ETL)

4.1.1 Fabrication of compact layer on FTO substrate

Three characterisations were done for the compact layer of TiO_2 which was spin coated on FTO glass, these are: XRD, FE-SEM and UV-vis spectroscopy.

XRD

Fig 4.1 shows the XRD plot of compact layer of TiO_2 spin coated on FTO substrate, After looking at the XRD plot and verifying the same from the JCPDS file, we can say that the TiO_2 deposited on the FTO substrate is of the Rutile Phase and is the desired one.

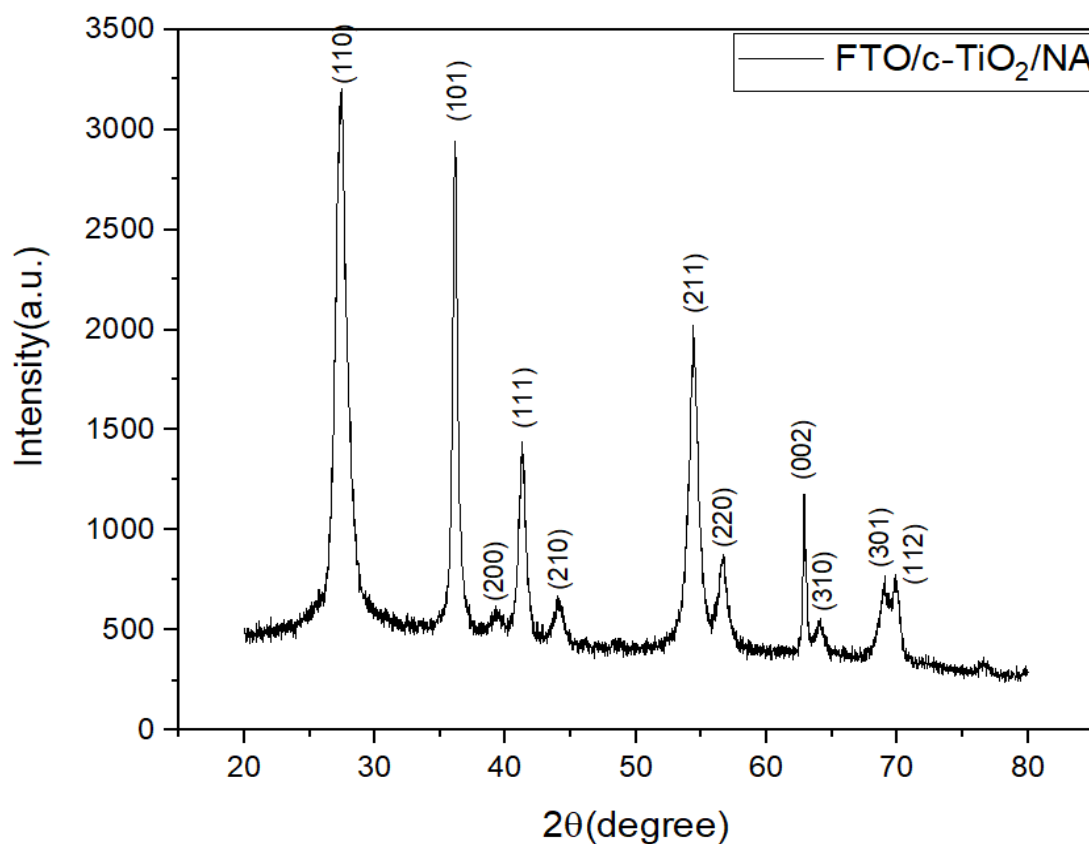


Fig 4.1 XRD plot of compact layer of TiO_2 spin coated on FTO glass

FE-SEM

Fig 4.2 shows the FE-SEM images of the compact layer. We can clearly see the thin film being formed on the FTO glass substrate.

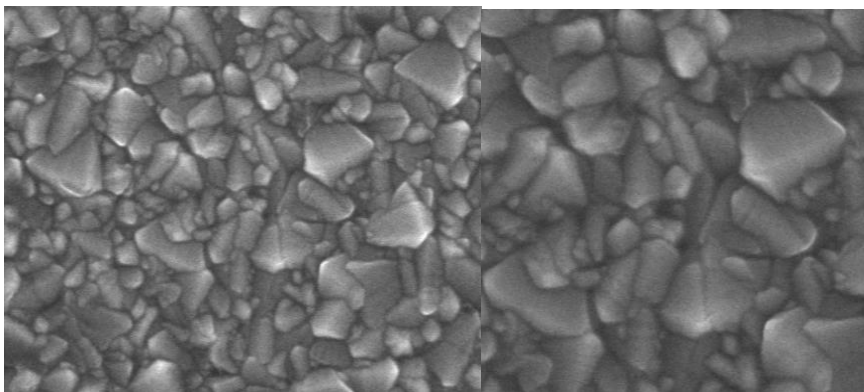


Fig 4.2 FE-SEM image of TiO₂ compact layer

UV - Visible Spectroscopy

Fig 4.3 shows the UV -Visible spectroscopy of TiO₂ compact layer. The graph shows the the energy band gap of the compact layer. This band gap is precisely what is required for the layer to function as an ETL layer.

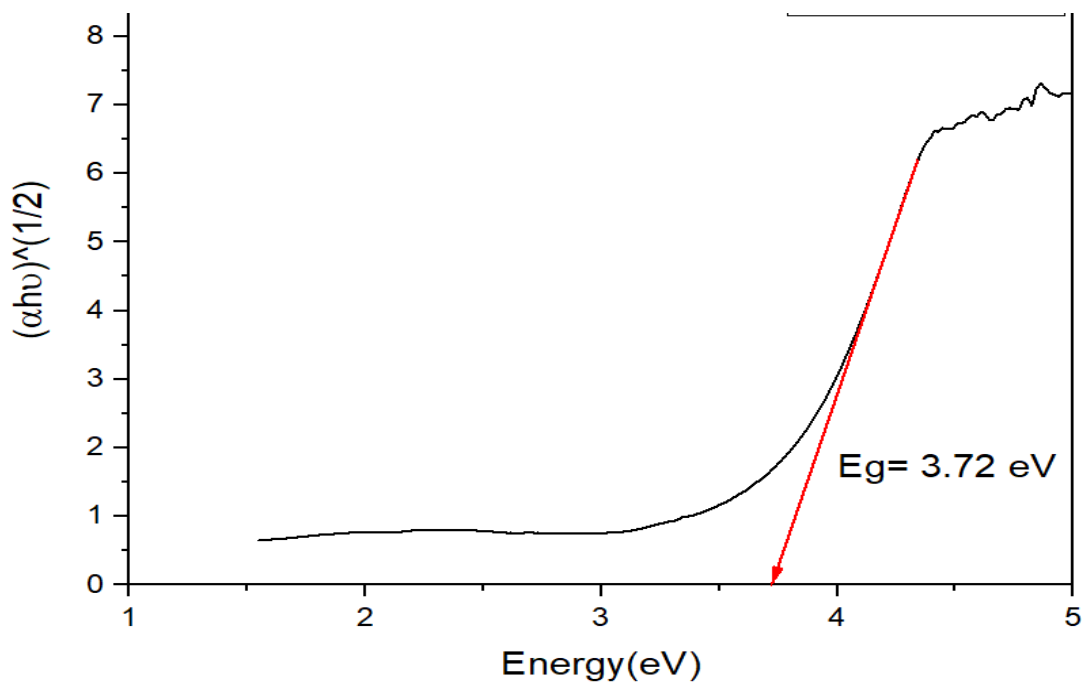


Fig 4.3 UV - Visible spectroscopy of TiO₂ compact layer

4.1.2 Fabrication of TiO₂ nanorods on top of the compact layer

The recipe and procedure followed for fabrication of nanorods is mentioned in the experimental section. For experimenting purposes, we have varied the concentration of DI Water and acid which were used to prepare the precursor solution, and also the time for which the autoclave was kept in the furnace. The concentration has been varied of DI Water + HCL as 10ml + 30ml, 20ml + 20ml and 30ml + 30ml. and the time for which the autoclave was kept in the furnace has been varied as 6, 8, 15, 17 and 20 hours.

The effect of these variations are as follows -

Effect of Variation of concentration -

After observing these variations, we came to the conclusion that DI Water and HCL taken in 1:1 is favourable for nanorods growth, the rest of the combinations are not viable, for example if we increase the amount of DI Water, it will increase the rate of hydrolysis of Titanium Butoxide, which will then lead to precipitation and settling down of TiO₂. And if we increase the acid concentration, it will suppress the hydrolysis of Titanium Butoxide, which will then lead to no formation of TiO.

So for further experimentation, we have taken the concentration of DI Water and HCL in 1:1

Effect of variation of time

By varying the time for which the autoclave was kept in the furnace, we can vary the diameter of the nanorods. As we decrease the time, the diameter of the nanorod decreases. **For 6 hours it is 31.133 nm. For 8 hours it is 82.71 nm, 15 hours it is 94.17 nm and for 17 hours it is 127.89 nm.**

For 6 Hours

XRD

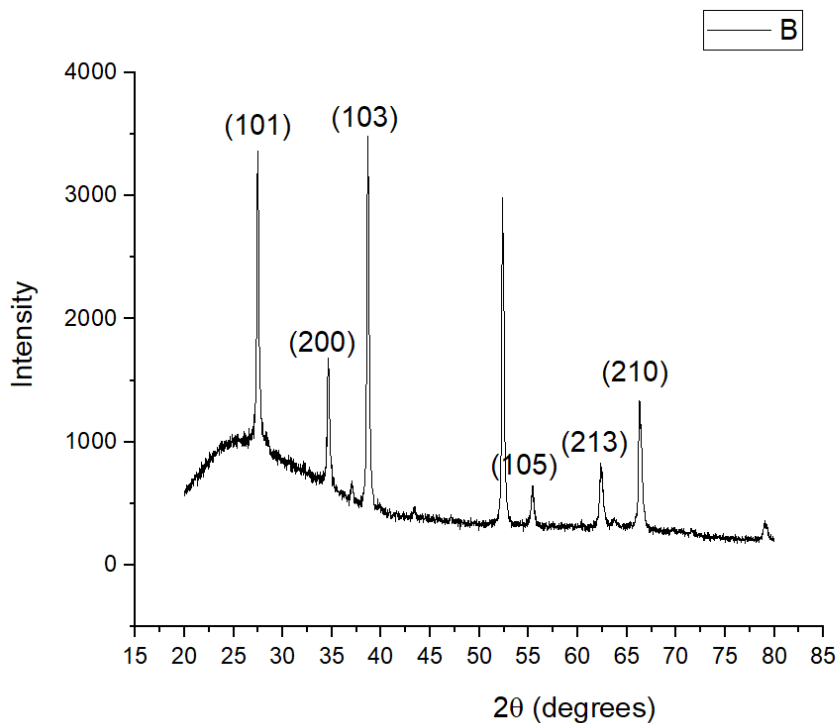


Fig 4.4 XRD plot of TiO₂ nanorods for 6 hours

UV-Vis Spectroscopy

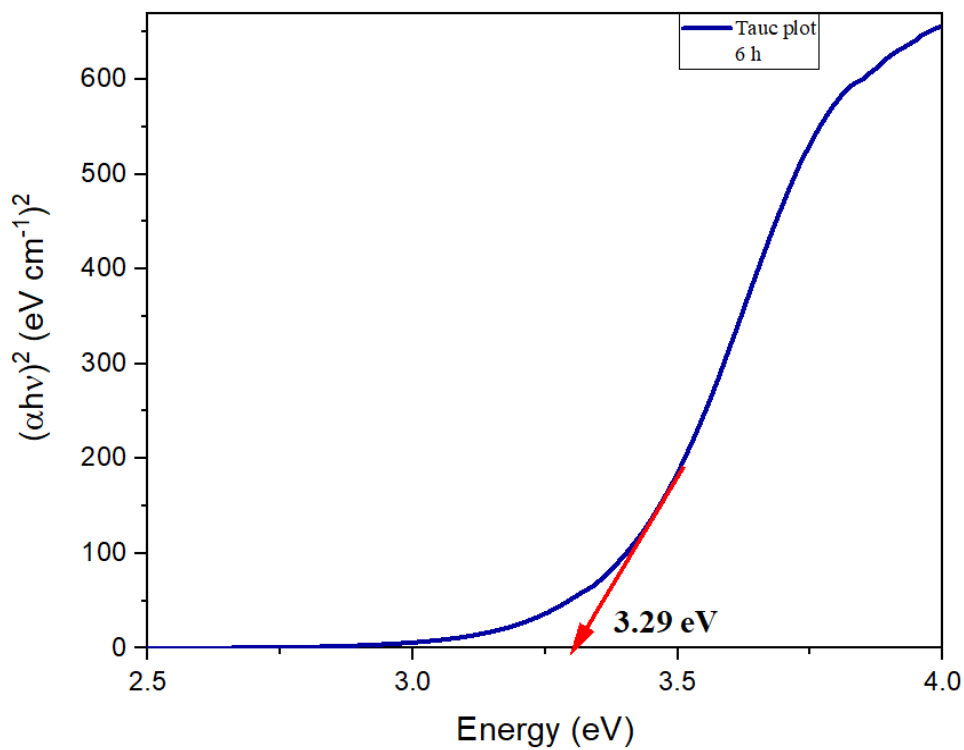


Fig 4.5 UV – Vis spectroscopy plot for TiO₂ nanorods for 6 hours

FE – SEM

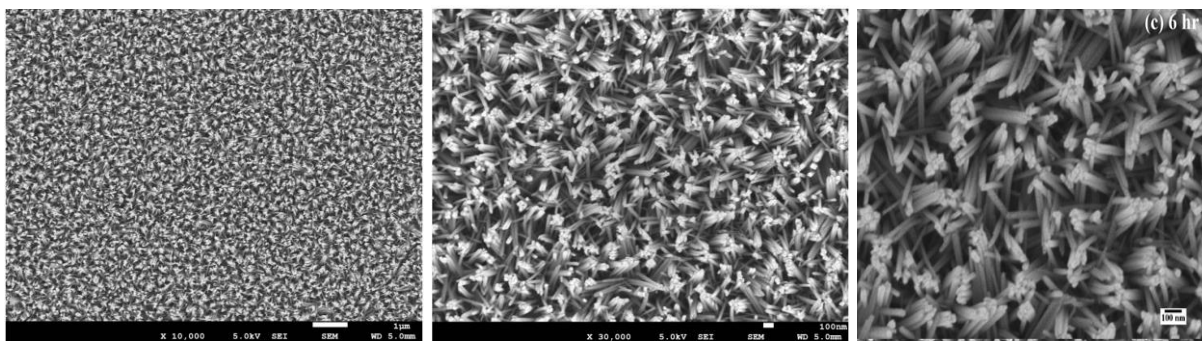


Fig 4.6 FE – SEM images of TiO₂ nanorods for 6 hours

For 8 Hours -

XRD

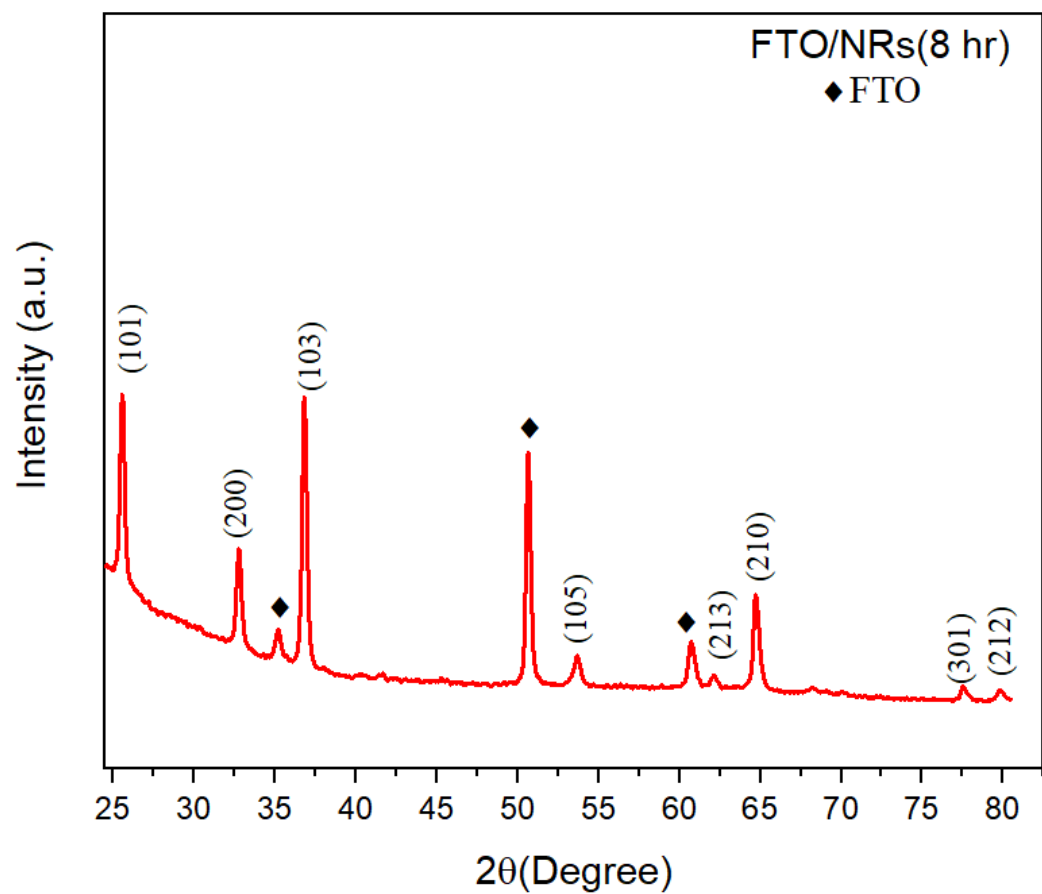


Fig 4.7 XRD plot of TiO₂ nanorods for 8 hours

UV - Visible Spectroscopy

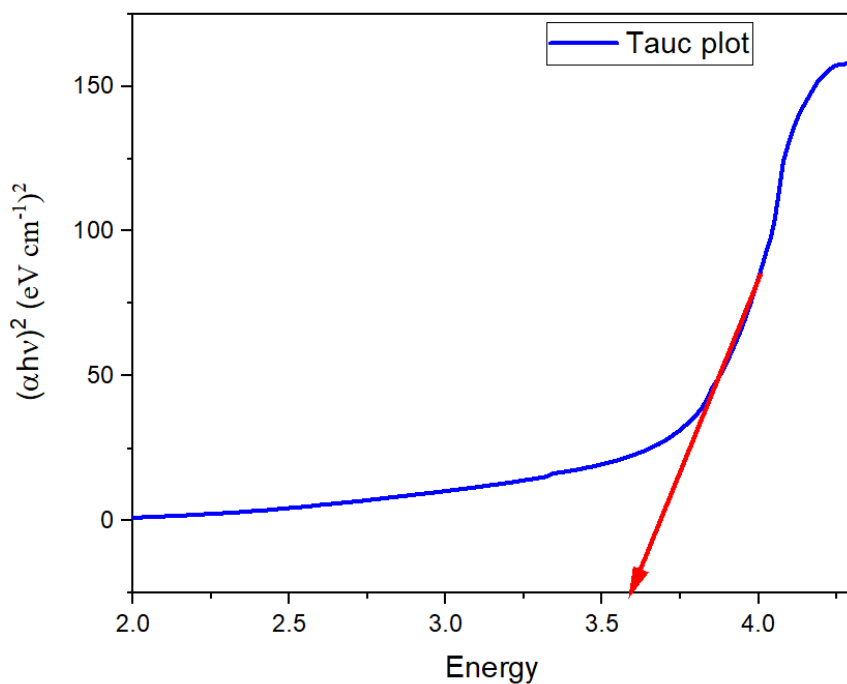


Fig 4.8 UV – Vis spectroscopy plot of TiO₂ nanorods for 8 hours

FE-SEM

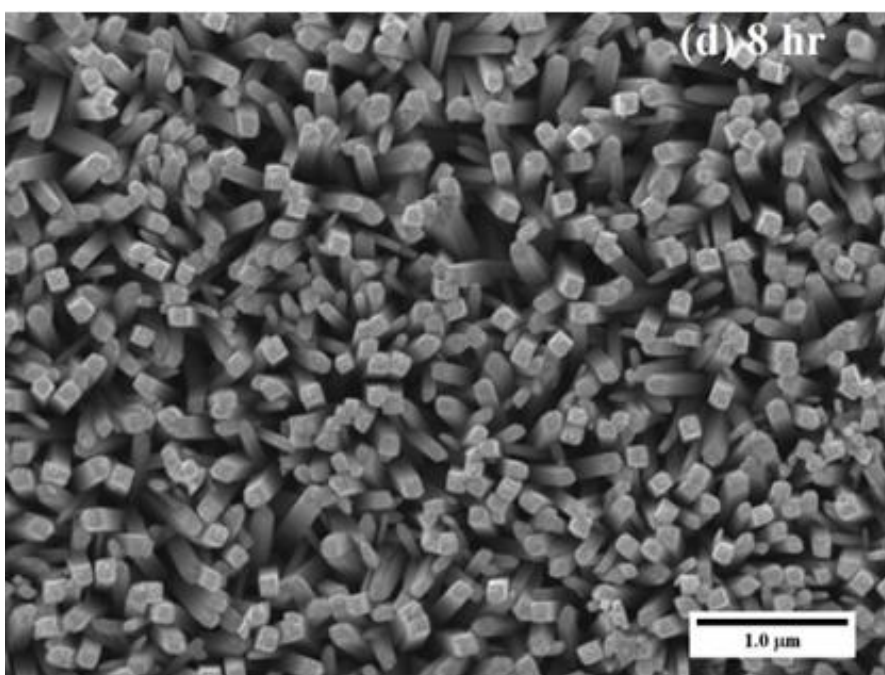


Fig 4.9 FE – SEM images of TiO₂ nanorods for 8 hours

By observing the FE-SEM images, we can conclude that for 8 hours, no substantial amount of nanorods were formed.

For 15 hours

XRD

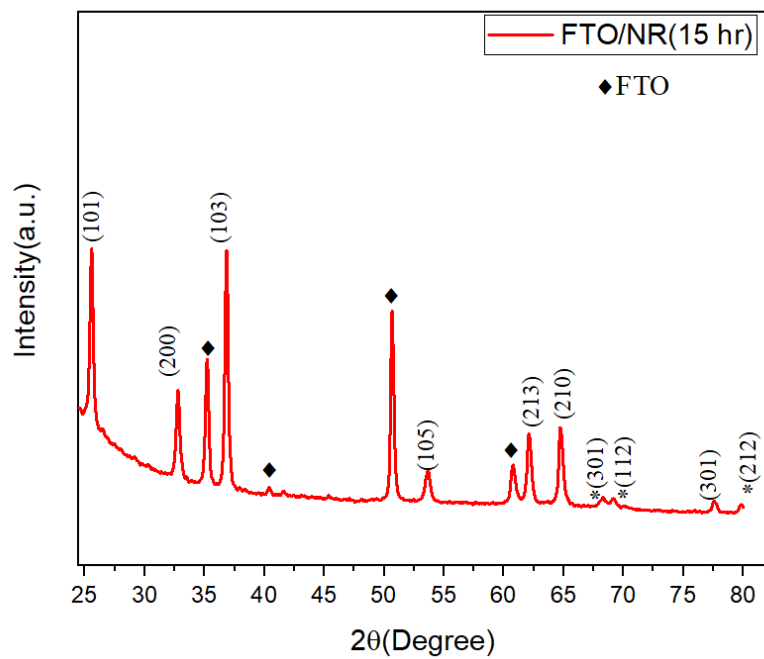


Fig 4.10 XRD plot of TiO₂ nanorods for 15 hours

UV -Visible Spectroscopy

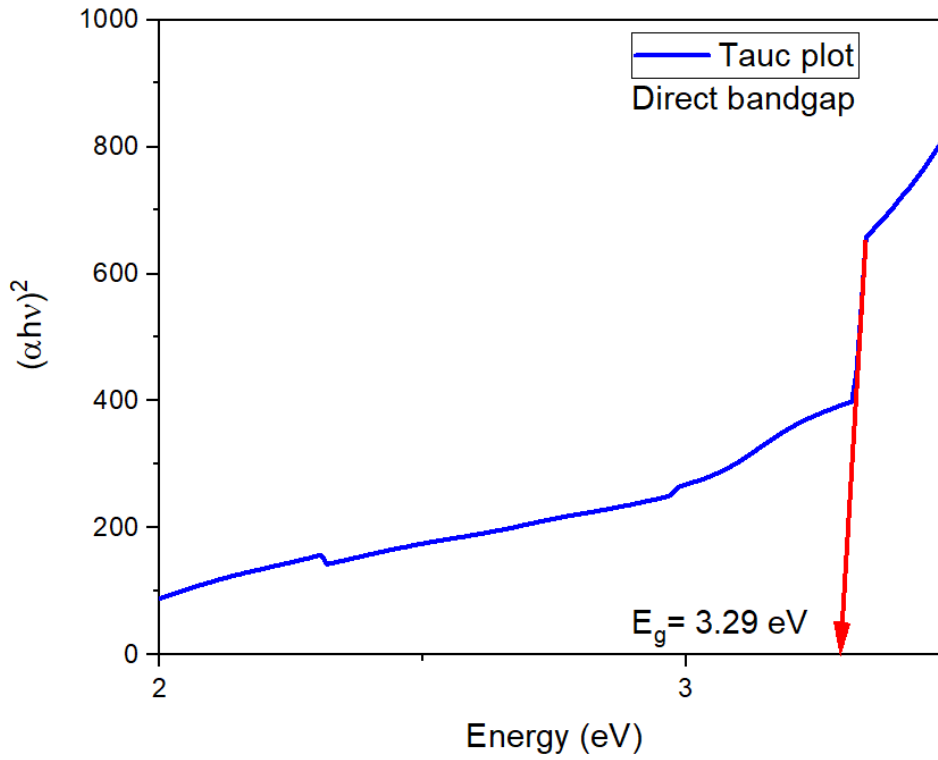


Fig 4.11 UV – Vis spectroscopy of TiO₂ nanorods for 15 hours

FE-SEM

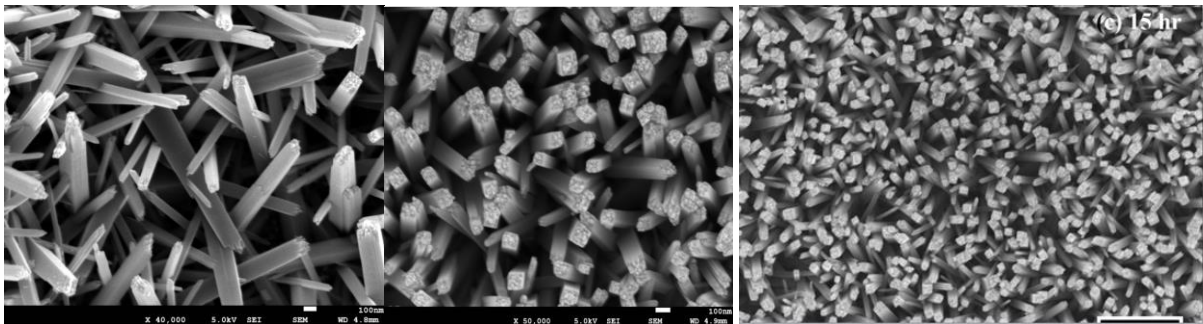


Fig 4.12 FE – SEM images of TiO₂ nanorods for 15 hours

The TiO₂ nanorods here are clearly visible.

For 17 Hours

UV -Visible Spectroscopy

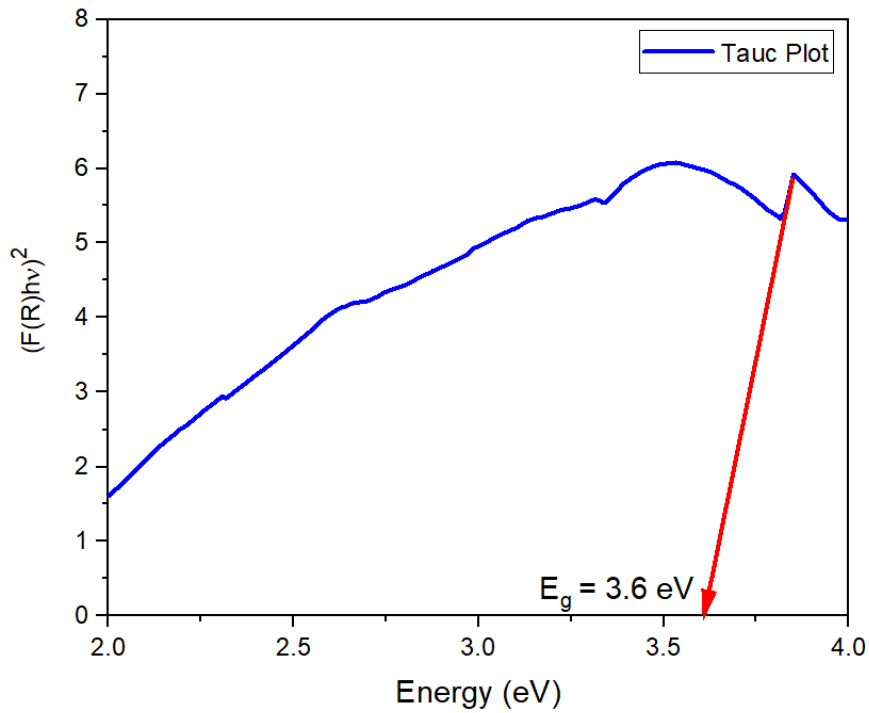


Fig 4.13 UV – Vis spectroscopy of TiO₂ nanorods for 17 hours

FE-SEM

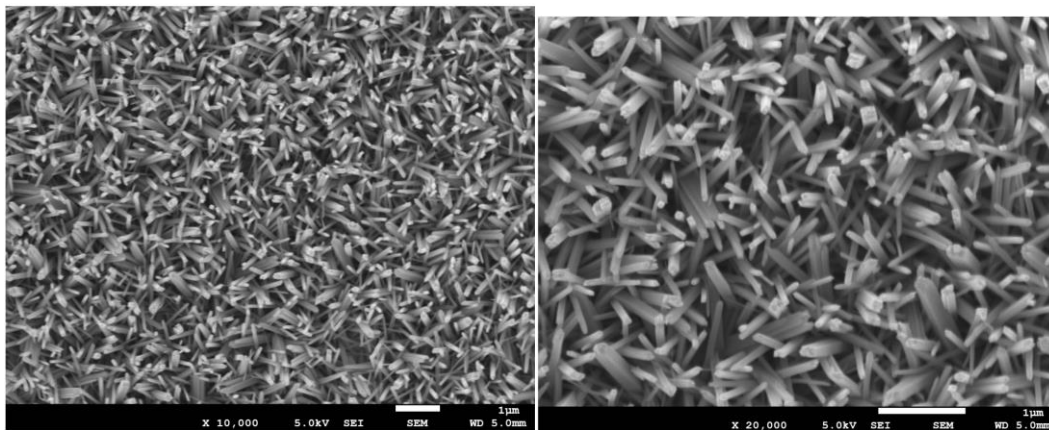


Fig 4.14 FE – SEM images of TiO₂ nanorods for 17 hours

After observing FE-SEM images of all the three samples (8 hr, 15 hr, 17 hr), we conclude that the most optimum temperature for formation of nanorods is 15 hours.

4.2 For Hole Transport Layer (HTL)

We have tried fabrication of HTL i.e. NiOx by two methods viz. by using Nickel Chloride (NiCl_2) and by using Nickel Nitrate ($\text{Ni}(\text{NO}_3)_2$).

4.2.1 By using Nickel Chloride (NiCl_2)

XRD

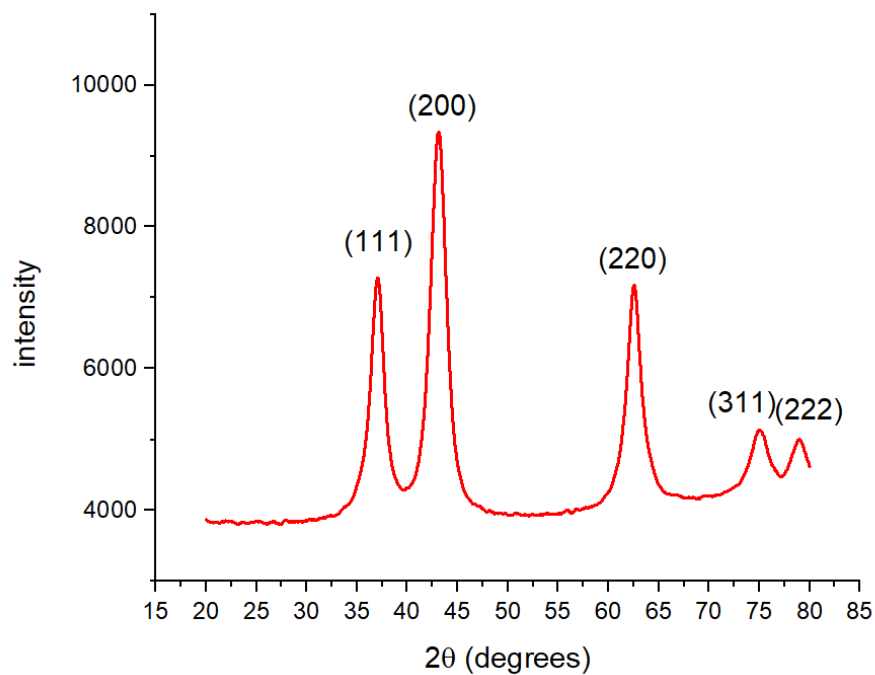


Fig 4.15 XRD plot of NiOx

FE-SEM

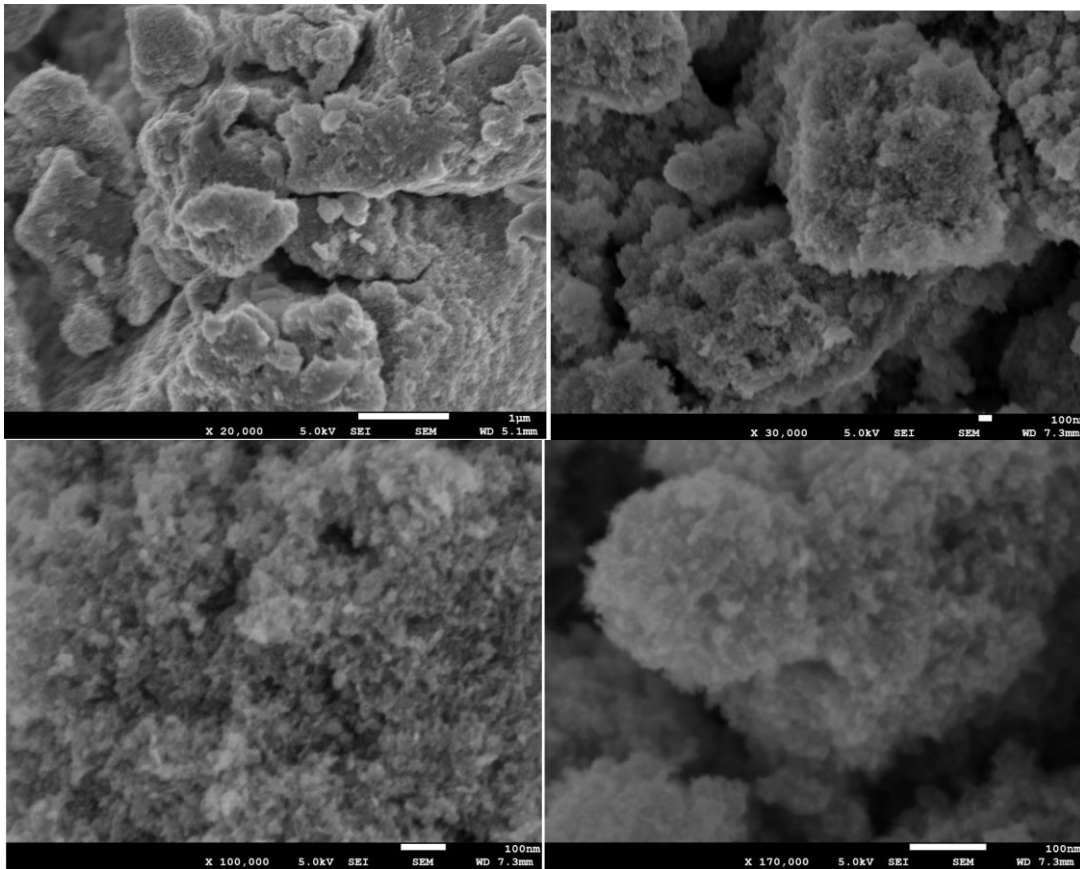


Fig 4.16 FE-SEM images of NiO

UV - Visible Spectroscopy

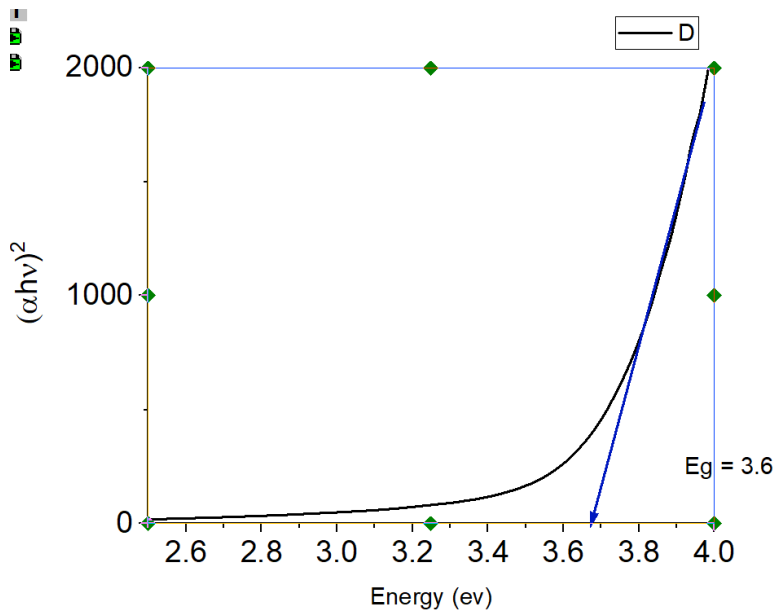


Fig 4.17 UV-Visible spectroscopy of NiOx sample

4.2.2 By using Nickel Nitrate $\text{Ni}(\text{NO}_3)_2$

XRD

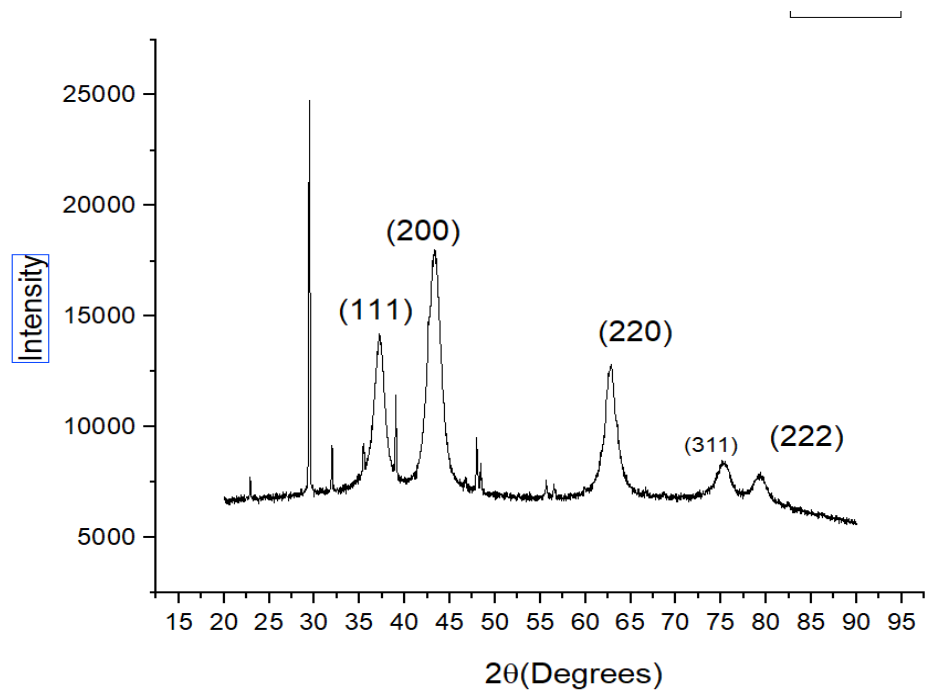


Fig 4.18 XRD plot of NiOx

UV - Visible Spectroscopy

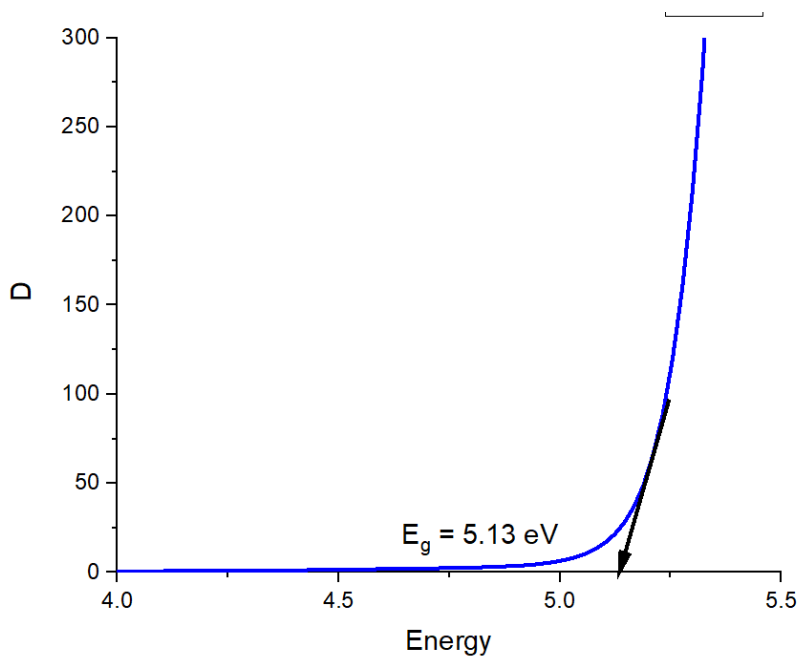


Fig 4.19 UV – Vis spectroscopy of NiOx

FE-SEM

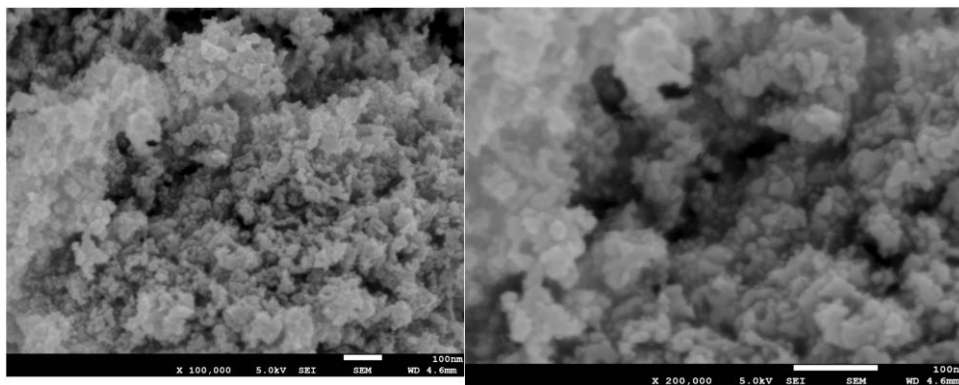


Fig 4.20 FE – SEM images of NiOx

4.3 Cell Fabrication for Degradation Controlled Properties

In all the thermal stability experiments performed, HTL and top electrode are not included. We heated the perovskite coated substrates on a hot plate at 150°C for different time durations and compared their performance. For the next experiment, we introduced a layer of PMMA coated without post-annealing between perovskite and NiOx. We saw an improvement in the performance compared to the standard architecture with that so we went on to test two different concentrations of PMMA. In the next experiment, we heated perovskite at 50°C with & without PMMA for different time durations going up till 14 hours where we saw an improvement in Voc in the cells heated overnight with PMMA compared to the reference. The accepted minimum standard for the operational temperature of solar cells is 85°C so we repeated our last experiment but this time the perovskite heating temperature was 100°C. This time also we saw a significant improvement in the performance when PMMA was used thus with our architectural changes we have made the cells less prone to thermal degradation. We used two characterization techniques i.e. FESEM and XRD on the substrates from our last two experiments. FE - SEM images have been analyzed for the morphological changes in perovskite structure and also the difference in lead content can be seen on the surface. With XRD plots the difference in peak intensity of lead iodide and perovskite the degradation in the perovskite layer was analyzed.

4.3.1 Adding a layer of PMMA between Perovskite and NiOx

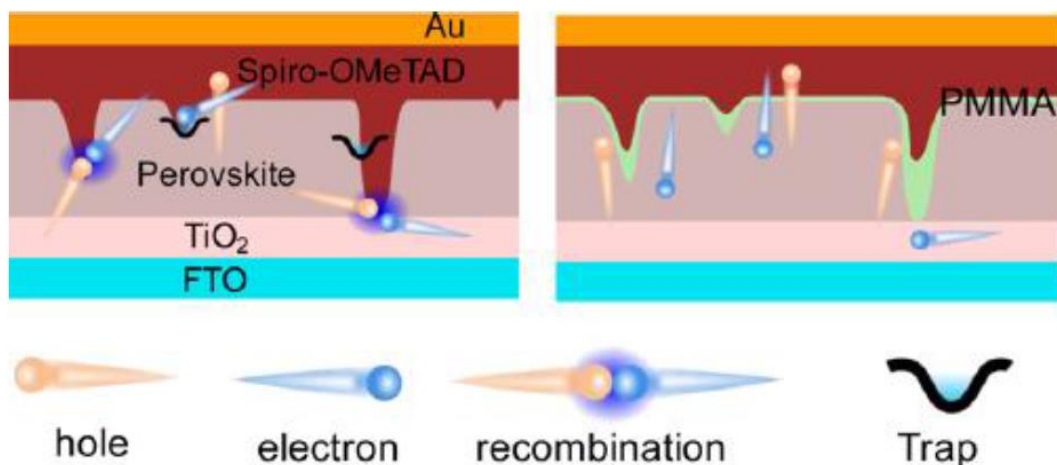


Fig 4.21 (a) PSC layered structure without PMMA (b) PSC layered structure with PMMA

We can see in the fig. 4.21(a) that the pinholes and grain-boundaries in the perovskite solar cells are filled by NiOx. This may cause a direct connection between the HTL & ETL which will reduce the built-in potential of the cell. The holes transporting through the HTL have a tendency to combine with the electrons because of these pinholes causing carrier recombination losses. Also, electron extraction is reduced because of non-radiative recombination due to the trap states. PMMA, on the other hand, fills the pinholes and grain boundaries and also since it is an insulator it prevents the shorting of ETL & HTL and passivates trap states which reduce the recombination losses and increases the Voc.

4.3.2 Heating the substrates with & without PMMA for various time durations at 50°C

Earlier cells with PMMA gave better results when post-annealed for 6 minutes compared to when they were not annealed. Considering that, in the following experiment after 6-minute post-annealing we heated some substrates for longer time durations at 50°C to see that if PMMA still shows better performance. Less thermal degradation of perovskite to PbI₂ occurs when PMMA is present which is evident from the XRD plot below. The diffraction peaks of the plot exactly match with the peaks from Jiang et al. whose recipe we had used for the PSC preparation. We can clearly see from the fig. 4.22 that the diffraction peak of PbI₂ at 12.6° is significantly lower when the PMMA is used and the peaks from the perovskite phases are quite higher which is evident of less thermal degradation with the use of PMMA. The peak for PMMA was not present, maybe because it is a very thin layer.

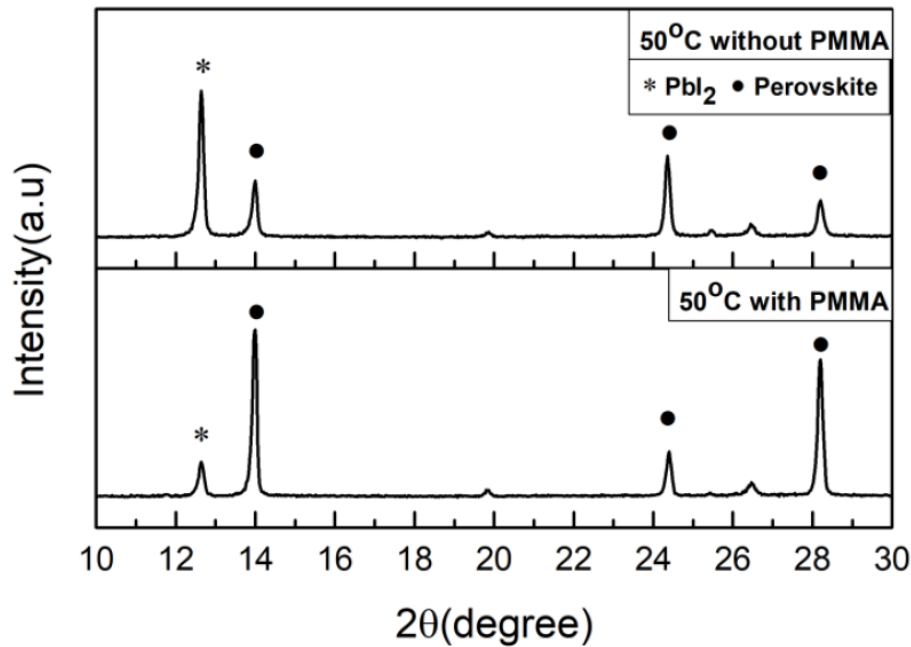


Fig 4.22 XRD plots of perovskite with & without PMMA heated at 50°C

The second reason is higher crystallinity and bigger grain size with the use of PMMA which can be seen in the FE-SEM images below that means the grain size has gotten smaller with thermal stress for reference cells. Bigger grain size means fewer grain boundaries which reduce the hindrance in charge-carrier transport. Also, the surface looks smoother from the passivation with PMMA which forms a better interface with NiOx thus enhancing the charge transport across it & reducing irradiative carrier recombination. The amount of white phase which is the PbI_2 is very high in the fig. 4.23(a) compared to the negligible amount in fig. 4.23(b) which is consistent with the XRD results.

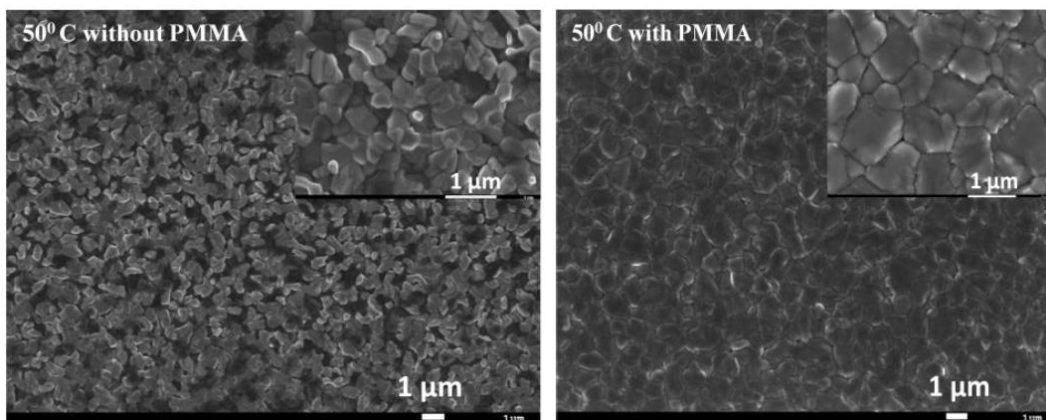


Fig 4.23 FE-SEM images: (a) Perovskite without PMMA heated for 14 hours at 50°C (b) Perovskite with PMMA heated for 14 hours at 50°C

4.3.3 Heating the substrates with & without PMMA for various time durations at 100°C

The accepted minimum standard for the operational temperature of solar cells is 85°C so we repeated our last experiment with temperature now being 100°C.

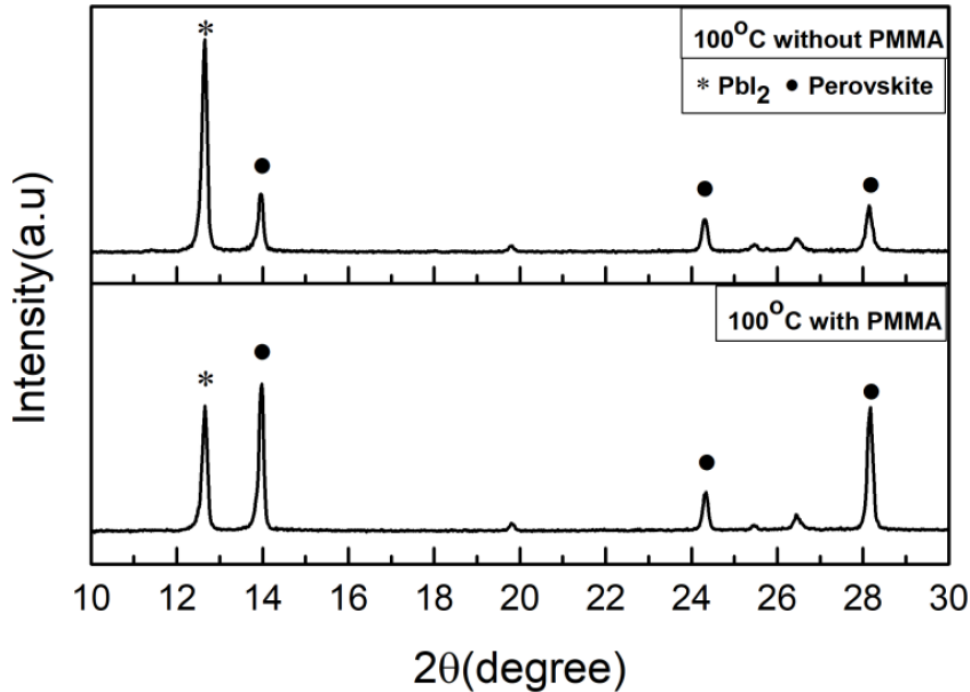


Fig 4.24 XRD plots of perovskite with & without PMMA heated at 50°C

From the fig. 4.24 we can see the decrease in intensity of diffraction peak belonging to PbI_2 PMMA is used but the decrement is not much which means a large amount of perovskite is still degraded. This can also be seen from the difference in the diffraction peaks perovskite phase which is not a lot. Still, the significant difference in performance can be because of the presence of this excessive PbI_2 in PMMA coated substrates as Jiang et al. has shown that a moderate residual of PbI_2 enhances performance by passivation of the surface or grain boundary defects but too much PbI_2 left in the perovskite can increase the ion movement which could lead to poor stability. In the SEM images below, it can be seen from the fig. 4.25(a) that most of the area is covered with a white phase of PbI_2 signifying that almost all of the perovskite on the surface is degraded. The amount of PbI_2 white phase visible in the fig. 4.25(b) is less and the amount black perovskite phase is more compared to fig. 4.25(a) which is consistent with the XRD results. Also, the grain size in fig 4.25(b) is bigger which means

that PMMA has helped perovskite to retain its crystallinity under thermal stress.

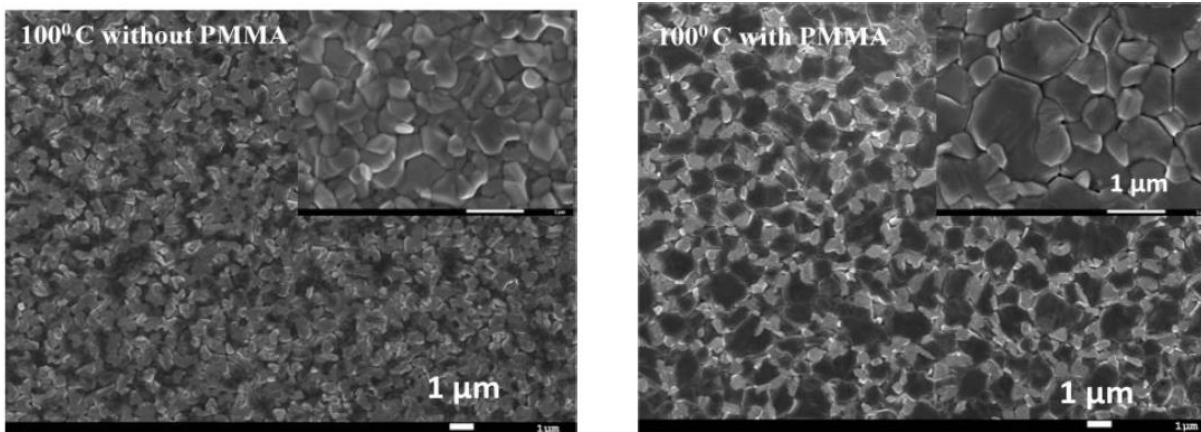


Fig 4.25 FE-SEM images: (a) Perovskite without PMMA heated for 14 hours at 100°C (b) Perovskite with PMMA heated for 14 hours at 100°C

CHAPTER 5

Conclusions and Scope for Future Work

The objective of the project was to fabricate a perovskite solar cell in ambient conditions. In order to do so, we need to fabricate different layers which when stacked together will form the solar cell. As Electron Transport Layer (ETL), we fabricated TiO_2 nanorods on top of the TiO_2 compact layer. TiO_2 nanorods were fabricated, first by variation of the acidity of the precursor solution, and second by varying the time for which the autoclave was kept in the furnace. On varying the acidity we observed that taking DI Water and 37% HCL in 1:1 will give the best result, any other variation will not be able to form nanorods. By varying time we observed that as we increase the time, the diameter of the nanorods also increases. As Hole Transport Layer (HTL), we fabricated NiOx, once with Nickel Chloride (NiCl_2) as precursor, and then with Nickel Nitrate ($\text{Ni}(\text{NO}_3)_2$) as precursor. After characterisation of both the samples, we concluded that $\text{Ni}(\text{NO}_3)_2$ is a better precursor for formation of NiOx, the reasons for the same could be that since nitrate can be fully displaced by NaOH as compared to Chloride which does not fully displaces.

For Degradation control, PMMA acts as a material for mitigating temperature degradation by avoiding the formation of PbI_2 resulting in avoiding direct contact between HTL and ETL thus increasing current flow and in turn efficiency

In this project, we have studied the effect of PMMA in reducing the thermal degradation of PSCs but a lot more experimentation is needed to get the best out of PMMA. The

process of spin coating PMMA can be optimized by trying out different RPMs, acceleration & time duration of spinning to get the best spin coating parameters which will give a layer thick enough to passivate the pinholes completely but it should not cause insulation between perovskite and HTL. Different post-annealing temperatures and time durations can be tested for optimal values. Also, the concentration of PMMA can be varied more. After all these optimizations I suspect that the thermal stabilizing properties of PMMA can be significantly enhanced. Also, this optimization can be performed on 2D- 3D perovskite-based PSCs which are highly moisture - stable so together the cell is less prone to degradation from humidity & temperature. Another thing that can be done is the change of HTL because it is coated directly over PMMA so it may affect the performance of the PSCs.

References

- [1] Mutalib, Muhazri Abd, et al. "Towards high performance perovskite solar cells: A review of morphological control and HTM development." *Applied Materials Today* 13 (2018): 69-82. Kojima, K. Teshima, Y. Shirai, T. Miyasaka, *J. Am. Chem. Soc.* 2009, 131, 6050.
- [2] H. S. Kim, C. R. Lee, J. H. Im, K. B. Lee, T. Moehl, A. Marchioro, S. J. Moon, R. Humphry-Baker, J. H. Yum, J. E. Moser, M. Gratzel, N. G. Park, *Sci. Rep.* 2012, 2, 591.
- [3] M. M. Lee, J. Teuscher, T. Miyasaka, T. N. Murakami, H. J. Snaith, *Science* 2012, 338, 643.
- [4] W. S. Yang, J. H. Noh, N. J. Jeon, Y. C. Kim, S. Ryu, J. Seo, S. I. Seok, *Science* 2015, 348, 1234.
- [5] D. Bi, C. Yi, J. Luo, J. D. Décoppet, F. Zhang, S. M. Zakeeruddin, X. Li, A. Hagfeldt, M. Gratzel, *Nat. Energy* 2016, 1, 16142.
- [6] W. S. Yang, B. W. Park, E. H. Jung, N. J. Jeon, Y. C. Kim, D. U. Lee, S. S. Shin, J. Seo, E. K. Kim, J. H. Noh, S. I. Seok, *Science* 2017, 356, 1376.
- [7] Jiang Q, Chu Z, Wang P, et al. Planar-structure perovskite solar cells with efficiency beyond 21%. *Adv Mater.* 2017; 29(46):1703852.
- [8] H. S. Kim, C. R. Lee, J. H. Im, K. B. Lee, T. Moehl, A. Marchioro, S. J. Moon, R. Humphry-Baker, J. H. Yum, J. E. Moser, M. Grätzel and N. G. Park, *Sci. Rep.*, 2012, 2, 591
- [9] Moehl, Thomas, et al. "Strong photocurrent amplification in perovskite solar cells with a porous TiO₂ blocking layer under reverse bias." *The journal of physical chemistry letters* 5.21 (2014): 3931-3936.
- [10] Basic Photovoltaic principles and methods- Solar Information module 6213

- [11] Mutalib, Muhazri Abd, et al. "Towards high performance perovskite solar cells: A review of morphological control and HTM development." *Applied Materials Today* 13 (2018): 69-82. Kojima, K. Teshima, Y. Shirai, T. Miyasaka, *J. Am. Chem. Soc.* 2009, 131,6050.
- [12] H. S. Kim, C. R. Lee, J. H. Im, K. B. Lee, T. Moehl, A. Marchioro, S. J. Moon, R. Humphry-Baker, J. H. Yum, J. E. Moser, M. Gratzel, N. G. Park, *Sci. Rep.* 2012, 2, 591.
- [13] J. Jung, D. L. Kim, S. H. Oh, and H. J. Kim, "Stability enhancement of organic solar cells with solution-processed nickel oxide thin films as hole transport layers," *Sol. Energy Mater. Sol. Cells*, vol. 102, no. Supplement C, pp. 103–108, Jul. 2012.
- [14] M. M. Lee, J. Teuscher, T. Miyasaka, T. N. Murakami, H. J. Snaith, *Science* 2012, 338, 643.
- [15] W. S. Yang, J. H. Noh, N. J. Jeon, Y. C. Kim, S. Ryu, J. Seo, S. I. Seok, *Science* 2015, 348, 1234.
- [16] "Pinhole-Free and Surface-Nanostructured NiO_x Film by Room-Temperature Solution Process for High-Performance Flexible Perovskite Solar Cells with Good Stability and Reproducibility" Hong Zhang, Jiaqi Cheng, Francis Lin, Hexiang He, Jian Mao, Kam Sing Wong, Alex K.-Y. Jen, and Wallace C. H. Choy
- [17] "New Method of Nickel Oxide as Hole Transport Layer and Characteristics of Nickel Oxide Based Perovskite Solar Cell" Loi Nguyen Old Dominion University
- [18] S. Ito, "Research Update: Overview of progress about efficiency and stability on perovskite solar cells," *APL Mater.*, vol. 4, no. 9, p. 091504, Sep. 2016.